

pubs.acs.org/JPCC Article

Room Temperature Migration of Ag Atoms to Cover Pd Islands on Ag(111)

Buddhika S. A. Gedara, Mark Muir, Arephin Islam, Dairong Liu, and Michael Trenary*



Cite This: J. Phys. Chem. C 2021, 125, 27828–27836



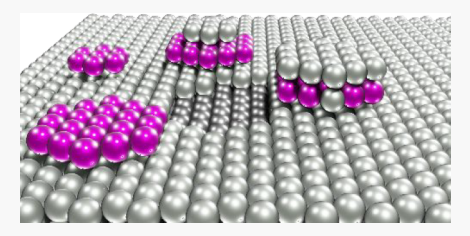
ACCESS I

Metrics & More

Article Recommendations

Supporting Information

ABSTRACT: The structures of Pd islands at three different Pd coverages (0.028, 0.064, and 0.150 monolayer (ML)) on Ag(111) were studied at room temperature with scanning tunneling microscopy (STM). While previous studies have shown that the structure and composition of Pd islands on Ag(111) change at elevated temperatures, we found that Ag atoms migrate to cover the Pd islands even at room temperature. These Ag atoms occupy sites in the middle of the islands, and second layer growth begins at these sites. The migration of Ag atoms leads to the formation of vacancy islands in the Ag(111) terraces. Upon annealing to 340 K, the majority of the Pd islands



are encapsulated by Ag atoms to form an Ag/Pd/Ag(111) structure. However, upon further annealing the composition of some islands at a Pd coverage of 0.150 ML changed to Ag/Ag/Pd/Ag(111).

1. INTRODUCTION

The optimum performance of a catalytic process can often be achieved with bimetallic catalysts. For example, PdAg catalysts are most effective for the partial hydrogenation of acetylene to ethylene by combining the high activity of Pd with the selectivity of Ag.¹ The catalytic properties of a bimetallic catalyst will depend on the atomic structure of the surface, which is likely to change during the course of the reaction, particularly under reaction conditions at elevated temperatures. However, structural changes are also possible at room temperature even in the absence of reactive gases. Our results confirm results reported by others for the Pd/Ag(111) system but reveal important new details.

Van Spronsen et al. used STM to show that 0.2 ML of Pd deposited on Ag(111) at room temperature formed mainly monolayer islands.2 Upon annealing to 400 K, Ag-capped PdAg alloy islands formed as well as vacancy pits in the Ag(111) layer. They further showed that exposure of the Pd/ Ag(111) surface to CO led to migration of Pd to the surface. Lim et al. used machine-learning molecular dynamics simulations to explore the details of the Ag migration and encapsulation of Pd islands on Ag(111).3 Their simulations were mainly done at a surface temperature of 500 K. O'Connor et al. reported that H_2 can dissociate on Pd islands on Ag(111) and that some of the resulting H atoms can spill over to Ag(111) sites.4 In contrast, at the very low coverages where Pd atoms are isolated in the topmost Ag layer, H atom spillover does not occur. 5 The coverage dependence of the hydrogen spillover is one of several reasons why the details of the coverage-dependent structure of Pd on Ag(111) are important to the catalytic function of this bimetallic system. Our work complements these previous studies in several ways. First, we find that Ag encapsulation of Pd islands readily occurs even at room temperature on the time scale of minutes. Second, we

report results at much lower Pd coverages than used by van Spronsen et al.² Third, we show that growth of the Ag layer on top of the Pd islands is nucleated at sites near the centers of the islands.

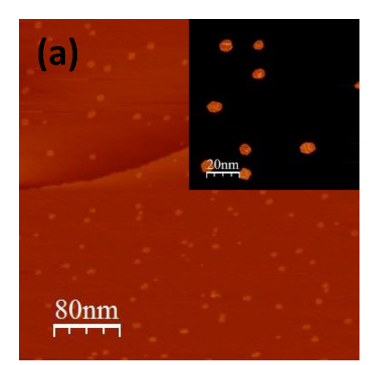
2. EXPERIMENTAL SECTION

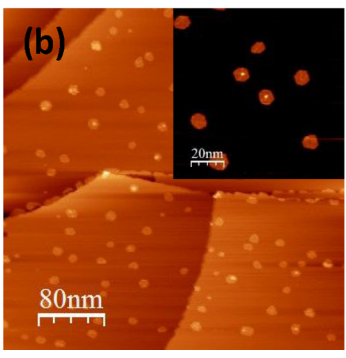
The experiments were performed in an ultrahigh vacuum chamber (UHV) with a base pressure of 1×10^{-10} mbar, and the STM images were obtained at room temperature (RT) with an Omicrom, GmbH, variable-temperature scanning probe microscope (VT-SPM) system. Images were acquired with Omicrom MATRIX software, and data processing was done with the WSxM program provided by Nanotech. The Ag(111) surface was cleaned by repeated cycles of sputtering with argon (3 \times 10⁻⁵ mbar, 1000 V) and annealing to \sim 700 K. The surface was verified to be clean by low-energy electron diffraction (LEED) and STM images (Figure S1). Palladium was deposited on Ag(111) via evaporation from a pure Pd rod (GoodFellow, 99.95%) by a triple electron beam evaporator (EFM 3T) with integral flux monitor at a rate of 1×10^{-3} ML/ s. The Pd coverage was determined directly from the STM images, and 1 ML corresponds to the Ag(111) atom density of 1.38×10^{15} atoms/cm². During Pd evaporation, the Ag(111) crystal was held at RT, and the background pressure never exceeded 3×10^{-10} mbar. The z-axis of the piezo scan tube was calibrated by using the height of monatomic steps on the

Received: October 5, 2021
Revised: November 11, 2021
Published: December 13, 2021









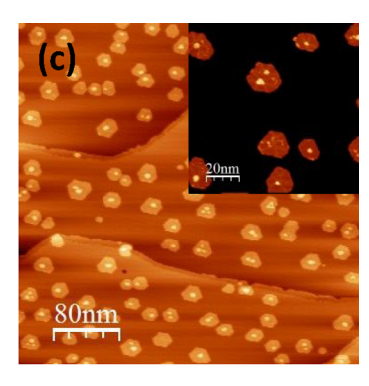
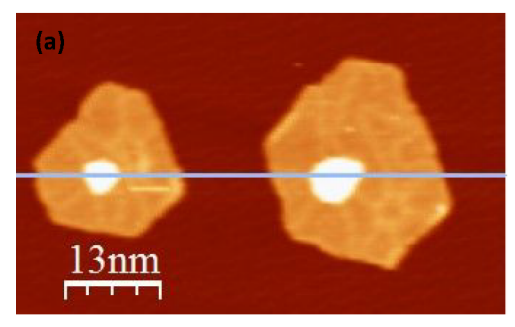
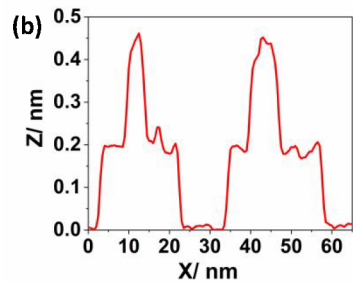


Figure 1. STM topographic images of (a) 0.028, (b) 0.064, and (c) 0.150 ML of Pd on Ag(111) in a 400×400 nm² area. Insets show the Pd islands on the terrace in a 100×100 nm² area. The number of Pd islands is independent of Pd coverage as shown in the insets, and the Pd island size increases upon increasing the coverage. Images were recorded at 0.20 nA and 2.0–1.0 V.





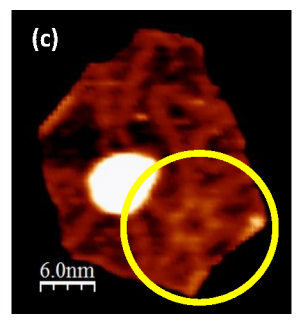


Figure 2. (a) Pd islands following deposition of 0.150 ML of Pd. (b) Height profile along the blue line in (a). Image was recorded at 0.2 nA and 2 V. (c) Enhanced contrast of the island on the left in (a) showing a hexagonal array that resembles stacking fault tetrahedra observed on Au(111).

Ag(111) surface (0.24 nm).⁷⁻¹⁰ Lateral calibration was based on the $22 \times \sqrt{3}$ reconstruction unit cell of Au(111).^{11,12}

3. RESULTS

a. Evolution of the Pd/Ag(111) Surface at Room Temperature. Figure 1 shows STM topographic images of 0.028 ± 0.005 (a), 0.064 ± 0.002 (b), and 0.150 ± 0.015 ML (c) of Pd deposited on Ag(111) at room temperature. The roughly hexagonal-shaped Pd islands are distributed across the Ag terraces and increase in diameter with increasing Pd coverage. O'Connor et al. also reported hexagonal Pd islands for 0.04 ML of Pd deposited on Ag(111) at room temperature.⁴ The diameters of the Pd islands for 0.028, 0.064, and 0.150 ML of Pd are 6.83 \pm 1.22, 10.55 \pm 2.15, and 15.04 ± 3.13 nm, respectively. However, the number of Pd islands is independent of Pd coverage, indicating that deposited Pd atoms migrate across the surface and attach to existing Pd islands. With increasing Pd coverage from 0.064 to 0.150 ML (Figure 1b,c insets) the onset of formation of a second layer is indicated by the appearance of bright spots near the centers of the islands. In the 0.150 ML Pd/Ag(111) image, nearly all the Pd islands possess second layer atoms.

Figure 2a shows an expanded view of two Pd islands with second layer atoms at a Pd coverage of 0.150 ML. Figure 2b shows a line profile taken across the two islands in panel a. The Pd island height appears to be about 0.2 nm in this case, although analysis of many small islands lacking second layer atoms shows the Pd island height is 0.150 \pm 0.019 nm. The apparent height of 0.2 nm in Figure 2b is likely due to the curvature of the tip being large compared to the distance from the island edge to the center. The height of 0.420 \pm 0.020 nm at the center above the second layer atoms is more than twice

the height of the first layer. On the basis of the monatomic step height of Ag (0.240 \pm 0.006 nm) and the monolayer Pd island height (0.150 \pm 0.019 nm), we conclude that the second layer is due to Ag encapsulation of the monolayer Pd island. Ideally, the sum of the monatomic step height of Ag and the height of the Pd island should be equal to the double-layer height. However, the lower height than expected on a purely geometric basis is attributed to different electronic properties of the Ag layer on the Pd islands from those of the Ag(111) surface. Encapsulation of Pd islands on Ag(111) by Ag atoms was observed with STM by van Spronsen et al.² for 0.20 ML Pd/Ag(111) deposited near RT and annealed to 405 K. We also concluded that Ag encapsulation occurred after annealing Pd/Ag(111) to 400-420 K based on reflection absorption infrared spectroscopy (RAIRS) and temperature-programmed desorption (TPD) of adsorbed CO.⁵ Patel et al. reported 0.459 nm high Pt-rich islands capped by displaced Ag atoms for a Pt/ Ag(111) surface at 300 K. Our results in Figures 1 and 2 show that the Ag encapsulation of Pd islands occurs at RT over short time periods (~30 min after deposition) and that second-layer growth is concentrated near the center of the Pd islands. We also scanned the Pd/Ag(111) surface after 48 h, and we observed that $\sim 30\%$ and $\sim 88\%$ of the Pd islands are encapsulated by Ag atoms at Pd coverages of 0.064 and 0.150 ML, respectively, while fewer than ~2% of the islands are encapsulated for 0.028 ML of Pd. STM topographic images of the surface after 48 h are given in Figure S2. Some aspects of our results are similar to those of de la Figuera et al., who used STM to show that Co deposition on Cu(111) at room temperature led to etching of the surface, 14 while Rabe et al. used low-energy ion scattering to show that Cu was gradually covered the Co layers.15

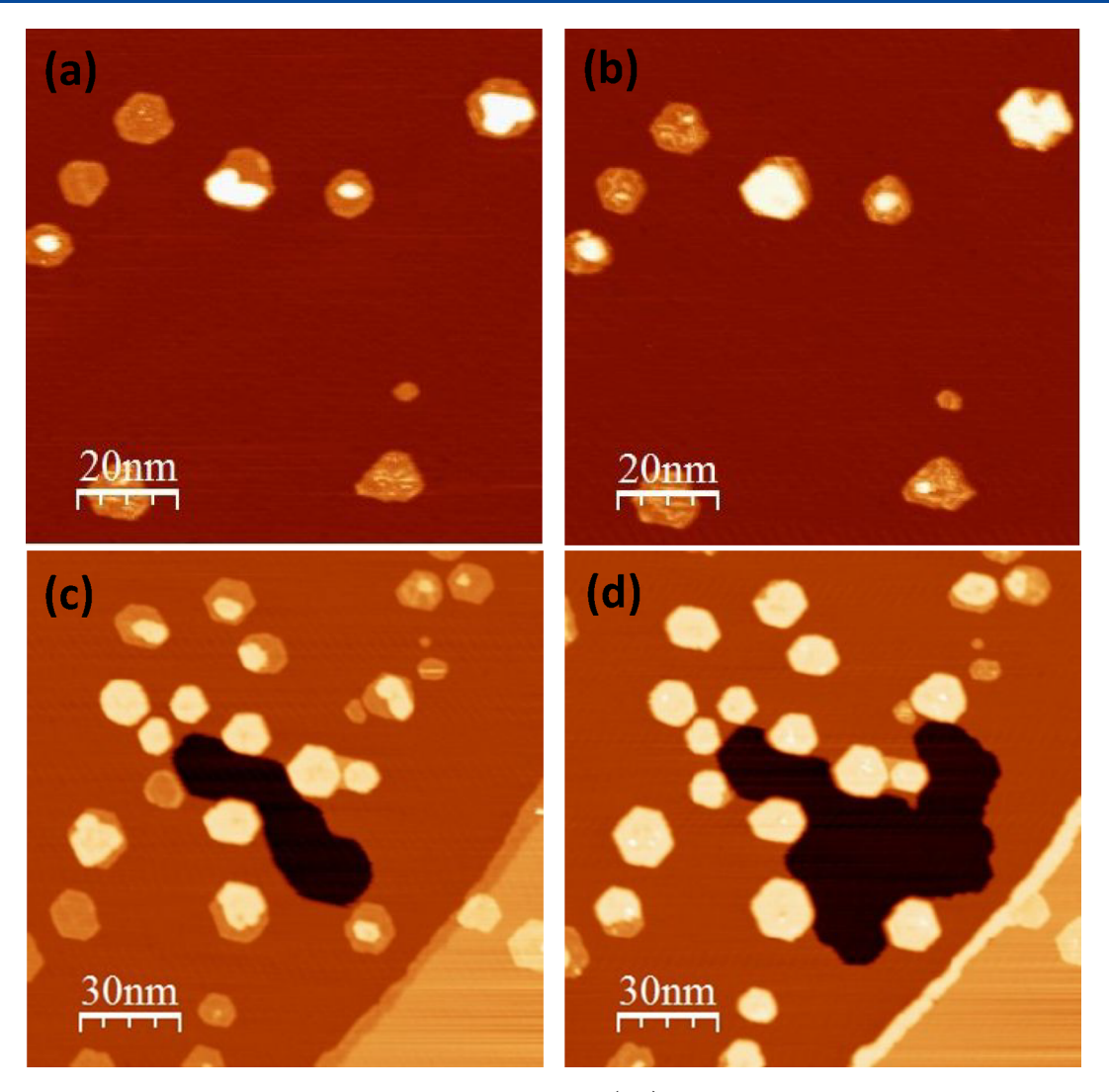


Figure 3. Images in the same area showing the evolution of structure with time. (a, b) 0.064 ML of Pd deposited on the Ag surface at t = 0 s and t = 3 h, respectively. (c, d) 0.150 ML of Pd deposited on the Ag surface at t = 0 s and t = 2.1 h, respectively. Images were recorded at 0.20 nA and 1.0 V.

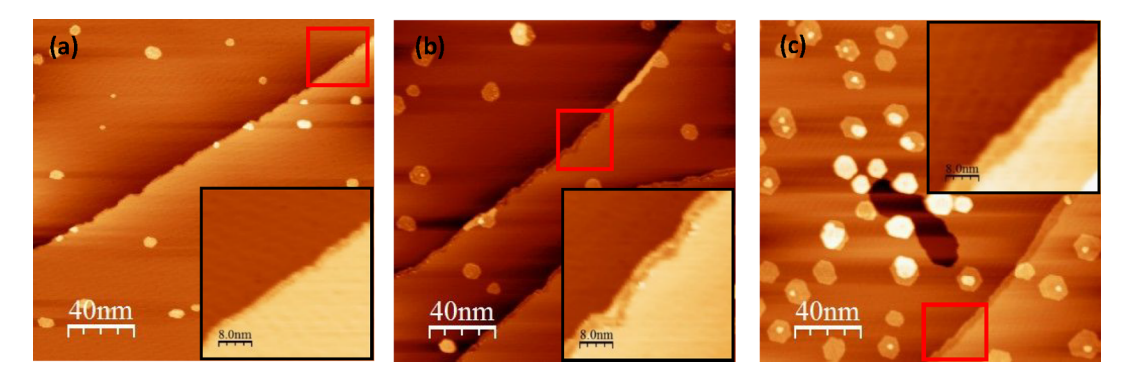


Figure 4. STM topographic images of (a) 0.028, (b) 0.064, and (c) 0.150 ML of Pd/Ag(111). Images were acquired at 0.2 nA and 1.0 V. Insets show the Pd-rich step edges in the red squares. Average widths of the Pd-rich steps are 4.17 ± 0.58 , 5.53 ± 0.71 , and 6.27 ± 1.04 nm at 0.028, 0.064, and 0.150 ML Pd coverages, respectively.

Several notable features of the islands are evident in the expanded scale images in Figure 2. The ridges within the Pd islands are similar to what is seen in moiré patterns in heteroepitaxial growth of Pd on Ni(111), Cu(111), and Au(111) surfaces. However, because of the small size of the islands, a periodic structure typically seen with moiré

patterns is not discernible in Figure 2. Patel reported similar features for Pd islands on Ag(111). Such ridges are also associated with dislocations, such as in the herringbone reconstruction of the Au(111) surface. In the latter case, a hexagonal arrangement of dots are occasionally observed at the intersection of six ridge lines with an appearance remarkably

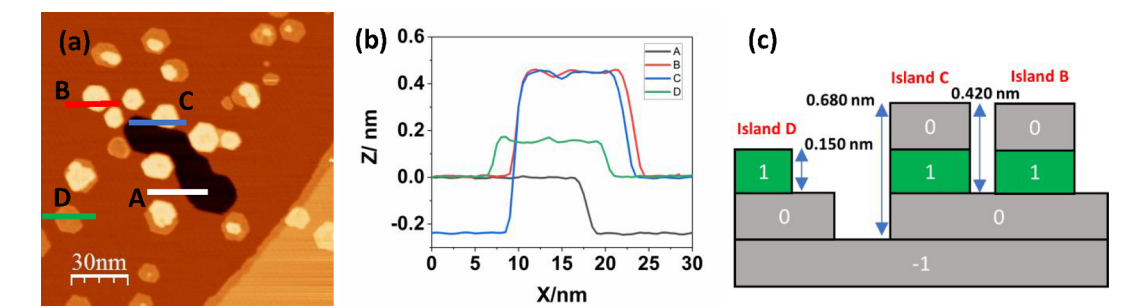


Figure 5. (a) 0.150 ML of Pd on Ag(111). Image was recorded at 0.20 nA and 1.0 V. (b) Height profiles along lines A, B, C, and D of image in (a). Line A shows monatomic step height of a vacancy island (0.240 \pm 0.006 nm), line B shows the height of a double-layer island (island B, 0.420 \pm 0.020 nm), line C shows the height of an island near the vacancy pit (island C, 0.680 \pm 0.005 nm), and line D shows the height of a Pd monolayer island (island D, 0.150 \pm 0.019 nm). (c) Schematic diagrams of the islands on Ag(111). 0 = surface Ag atoms, 1 = Pd atoms, and -1 = subsurface Ag atoms.

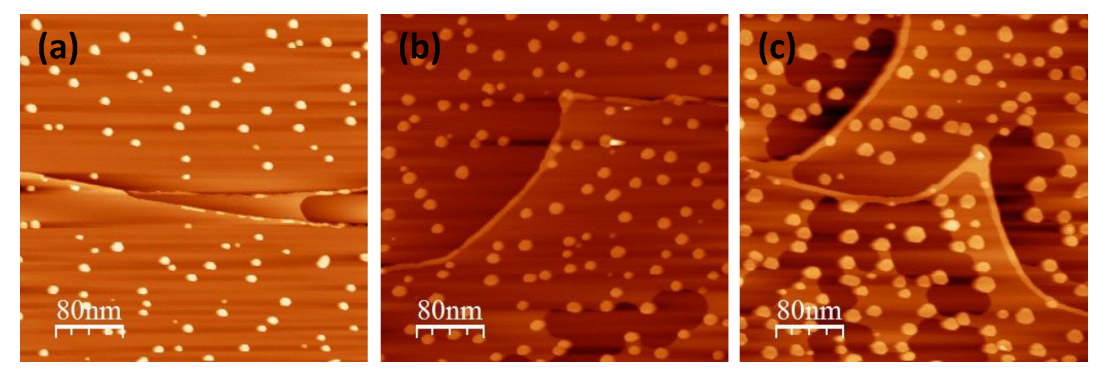


Figure 6. STM topographic images after annealing at 340 K for Pd coverages of (a) 0.028, (b) 0.064, and (c) 0.150 ML. Images were recorded at 0.20 nA and 2.0–1.0 V.

similar to what we observe within the yellow circle in Figure 2c. ²⁰ In the Au(111) case, these features were identified as stacking fault tetrahedra (SFT). ²⁰ Stacking fault tetrahedra also readily form on Ag(111), and on both Au and Ag the SFT display electronic properties different from the surrounding metal. ²¹ Regardless of whether or not the defect seen in Figure 2c is a SFT, it appears that the Ag atoms that migrate to the top of the Pd islands nucleate at such sites. As these defects occur near the middle of the Pd islands, growth of the second layer of Ag begins near the island centers.

Figure 3 shows how the 0.064 and 0.150 ML Pd/Ag(111) surfaces change over periods of 3 and 2 h, respectively. Figure 3a,b reveals that Ag atoms preferentially add to Pd islands already possessing second-layer atoms. Figure 3c,d shows a vacancy pit next to the Pd islands, which increased in area by a factor of 2.6 over 2 h and was accompanied by an increase in the number of second layer atoms. The Ag atoms that add to the Pd layer at the Ag(111) step edge seen in Figure 3c appear with the same brightness in Figure 3d as the Ag-capped Pd islands. A comparison of the images of 0.064 and 0.150 ML of Pd in Figure 3 suggests that second layer growth is faster for Pd islands near vacancy pits, presumably because of the shorter path the Ag atoms need to follow.

Additional information about the Pd that concentrates at the Ag(111) step edges is provided by the images in Figure 4. The appearance of the step edges can be attributed to Pd atoms exchanging places with Ag atoms at the ascending step edges. Such atom exchanges to form alloy brims at step edges have been reported for PtCu, 22 PtAg, 13 PdCu, 23,24 RhCu, 25 and PbCu. Because of the large difference in surface free energy between Pd (1.7 J m^{-2}) and Ag (1.1 J m^{-2}) , exchange of Ag

for Pd is thermodynamically favored. The size of the alloy brims for PtCu, PtAg, and PdCu depends on the size of the lower terrace, from which the authors of those papers conclude that the lower terrace acts as a catchment area for the deposited metal, whereas in PbCu, the width of the Pb seam is independent of the terrace width, indicating that diffusing Pb can overcome the potential barrier at the step edges. Although we observe that the brim width increases with Pd coverage, we have insufficient data to establish a clear correlation between lower terrace width and brim width. Figure S3b shows a line profile at a step edge for 0.150 ML of Pd. The height near the step edge along line B in Figure S3 is 0.15 nm. This height is the same as the height of a Pd island on the Ag(111) terraces.

Figure 5a is the same image as in Figure 3c, and Figure 5b shows line profiles across various locations in the image. Line A in Figure 5b drops by 0.240 ± 0.006 nm, indicating that the depressions are caused by Ag vacancies formed by Ag atoms that diffuse to the adjacent Pd islands. According to our line profiles, the height of the double-layer island is 0.420 ± 0.020 nm (same height as the center portion of the islands in Figure 2b). From these line profiles, we conclude that the composition of this double-layer island is Ag/Pd/Ag(111).

b. Effect of Annealing Temperature. Figure 6 shows STM topographic images of 0.028, 0.064, and 0.150 ML of Pd/Ag (111) annealed to 340 K. At each coverage, after 10 min of annealing, 98% of the Pd islands became double-layer islands and Ag vacancy pits formed. Because the 340 K anneal causes all the Pd islands to be covered by a second layer, for the larger islands at higher Pd coverages, more Ag must be supplied from the topmost Ag layer, and therefore the size of the vacancy pits increases.

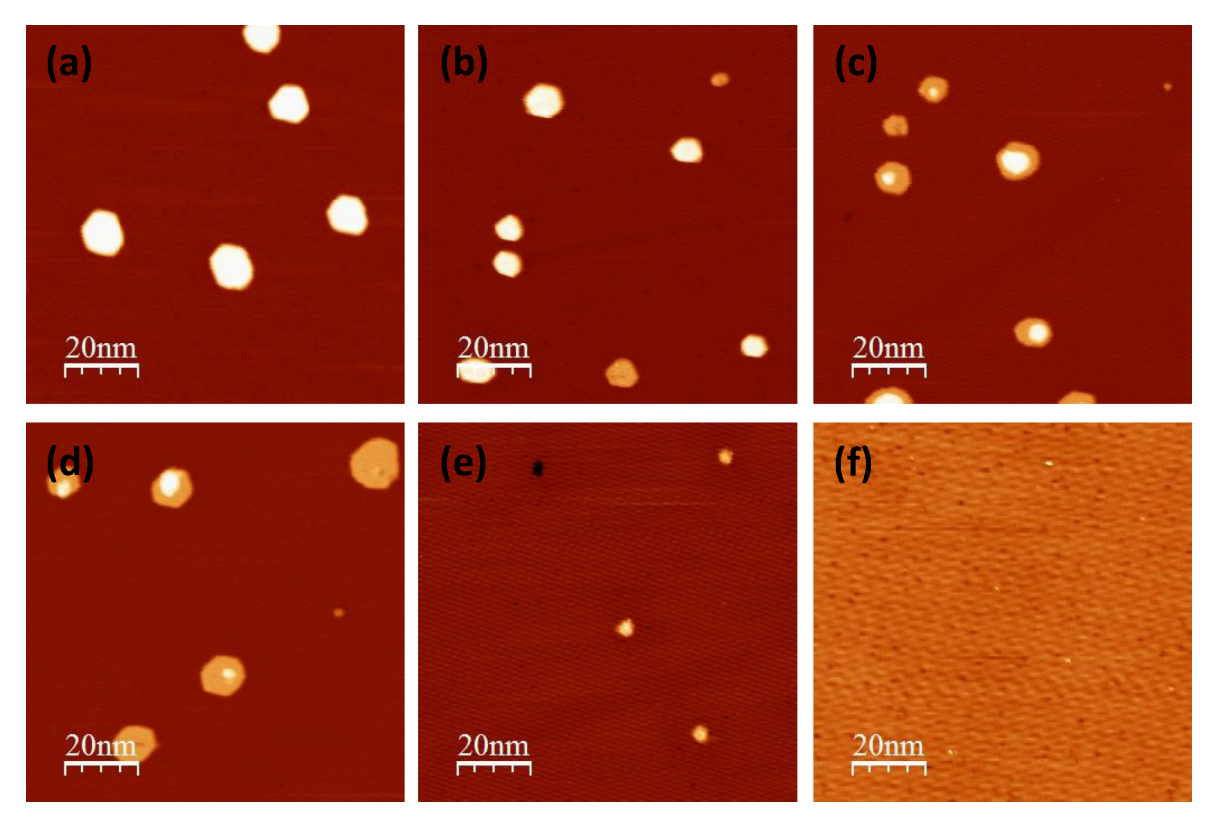


Figure 7. STM topographic images of 0.028 ML of Pd on Ag(111) annealed to (a) 340, (b) 390, (c) 420, (d) 440, (e) 450, and (f) 470 K. Images were recorded at 0.20 nA and 1.0 V.

Figure 7 shows the evolution of the 0.028 ML Pd/Ag(111) surface with increasing annealing temperature. Annealing the surface to 340 K gives rise to almost exclusively double-layer Pd islands while annealing to 420 K seems to show the reverse effect. Further annealing to 450 K shows a surface consisting of isolated clusters of atoms. Although not evident in the STM images, we⁵ showed that annealing to 420 K for 1 min produced a surface with both isolated Pd atoms (based on a PdC-O stretch at the atop site observed with RAIRS) and Ag encapsulation over the remaining Pd sites (as evidenced by an enhanced intensity of the AgC-O stretch). Figure 7f shows that annealing to 470 K results in a surface that is largely flat, consistent with Pd diffusion below the surface. Images were also acquired for surfaces with Pd coverages of 0.064 and 0.150 ML after annealing to the same temperatures as used in Figure 7 and are presented in the Supporting Information. At the higher Pd coverages, there is more complete encapsulation of the Pd islands by Ag and a greater variety of island structures. These include three-layer islands with a composition of Ag/ Ag/Pd/Ag(111) and double-layer Ag islands on top of Pd islands that have receded into the Ag(111) surface. A summary of the island types inferred from the images presented here and in the Supporting Information is presented in Table 1, which follows the scheme used in other recent publications.

4. DISCUSSION

The larger surface free energy of Pd (1.7 J m^{-2}) than of Ag $(1.1 \text{ J m}^{-2})^{27}$ makes any structure in which Pd is not below the topmost atomic layer of Ag(111) thermodynamically unstable. Thus, after annealing to sufficiently high temperature, Pd will migrate into the Ag bulk. The structures observed following Pd deposited at room temperature then reflect the kinetics of

various processes as the system relaxes toward the equilibrium structure. The observation that the size of the islands but not their number increases with Pd coverage indicates fast diffusion of Pd atoms on the Ag(111) terraces to existing Pd islands. At the same time, Pd atoms attach to ascending Ag step edges and can exchange with Ag atoms leading to Pd-rich brims on the upper terrace, as also seen by Patel et al. for Pt on $Ag(111)^{13}$ and in other systems. In the reverse situation, exchange of Pd by Ag for Ag deposited onto a Pd(111) surface would not be expected at the Pd steps as this would not lower the surface energy. There is no evidence for such exchange in the STM images of Engstfeld et al. for Ag deposited on Pd(111) at room temperature.²⁸ Similarly, while Ag atoms are expected to attach to the edges of Pd islands, this may be only a transient structure not detectable with STM before the Ag atoms migrate to the top of the islands. The edges of the vacancy islands in the Ag(111) surface are structurally similar to the Ag step edges, so exchange of Ag for Pd might be expected to occur there. However, these vacancies only form after the deposited Pd atoms have aggregated into islands followed by growth of the vacancies, so no Pd is deposited into the bottom of the pits.

The compact shape of the hexagonal Pd islands reflects the higher thermodynamic stability achieved by minimizing the perimeter-to-area ratio of the islands. However, this shape is not dictated by the differences in surface free energy alone, as Pt $(2.2~\mathrm{J~m^{-2}})^{27}$ has an even higher surface free energy than Pd, yet highly irregular shapes were observed for Pt islands on Ag(111) after deposition at 300 K. To achieve the thermodynamically favored shape, barriers for migration of metal atoms around the island perimeters must be sufficiently low. At 300 K, these barriers are evidently higher for Pt than for Pd. In general, from the earliest STM studies of metal-on-

Table 1. Summary of Annealing Experiments

Coverage/ ML	Pd island size/ nm	Composition of the islands			
		340 K	390 K	420-450 K	470 K
0.028	6.83	0 1 0 -1	0 1 0 1 1 -1	0 1 0 -1	0 1 -1
0.064	10.55	0 1 0 -1	0 1 0 1 1 -1	0 1 0 -1	0 1 -1
0.150	15.04	0 1 0 -1	0 1 0 -1	0 0 1 0 1 0 1 -1	0 1 0 -1
		0 0 1 0 -1	0 0 1 0 -1	0 0 0 0 1 0 1 0 1 -1	0 0 1 0 -1

^aNote: 0 = surface Ag atoms, 1 = Pd atoms, and -1 = subsurface Ag atoms.

metal growth, fractal-shaped islands have been observed for low deposition temperatures but compact islands at higher temperatures. For example, in the homoepitaxial growth of Pt on Pt(111), a deposition temperature of 200 K leads to dendritic islands but compact islands at 455 K. 29

Further insight into the processes responsible for the behavior observed here can be gained by comparing our results with the molecular dynamics simulations of Lim et al. of the evolution of the structure starting with hexagonal single-layer Pd_{91} islands on Ag(111).³ While Lim et al. address issues relevant to our observations, their Pd_{91} islands are much smaller than the ones we observe, which contain thousands of Pd atoms. Also, their simulations assumed a surface temperature of 500 K, which may enable processes to occur that do not occur at lower temperatures. Consequently, there may be experimentally observed effects that cannot be accounted for based on their Pd_{91} islands. The simulations of Lim et al. revealed four distinct stages of restructuring: (1) Pd–Ag place exchange, (2) formation of a PdAg alloy layer, (3) Ag pop-out

and vacancy pit growth, and (4) layer-by-layer Pd dissolution.³ The first three stages result in the encapsulation of the Pd islands by Ag atoms and simultaneous growth of the vacancy pits that are so prominent in our STM images. In stage 1, Ag atoms exchange with Pd atoms at the edges of the Pd islands, leading to islands decorated with Ag atoms. The Ag atoms can migrate from the island edges into the island interiors to form a two-dimensional PdAg alloy. Engstfeld et al. found that PdAg surface alloys formed for Ag deposited onto Pd(111) at room temperature but only after annealing to 800 K, suggesting a fairly high kinetic barrier for alloy formation.²⁸ In their room temperature STM images, the Ag and Pd atoms of the alloys were easily distinguished. If alloy formation occurred in our experiments, it presumably involved geometric and/or electronic differences between Ag and Pd that were generally too subtle to detect.

The barrier for the pop-out of a Ag atom from a terrace site is high but is lower next to a Pd island as attachment to the island edge stabilizes the final state. This is consistent with the

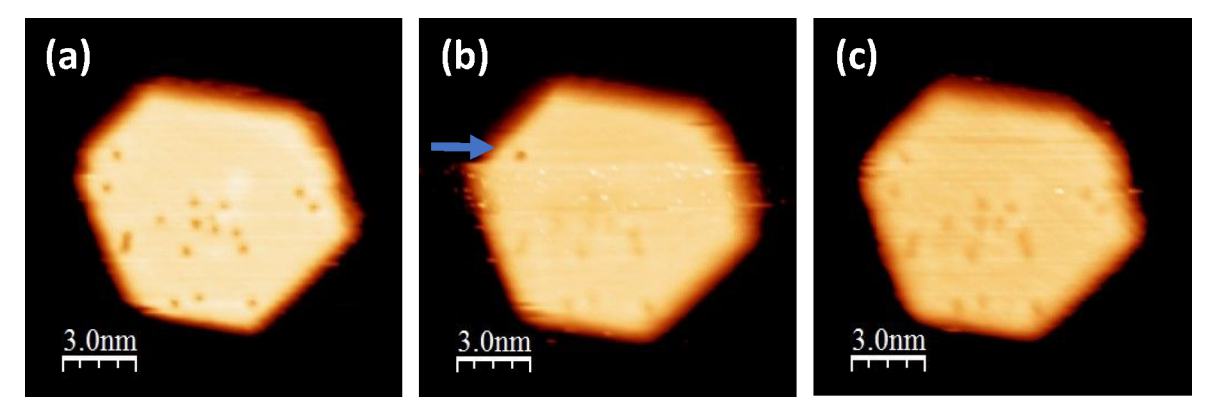


Figure 8. STM topographic images of a Ag encapsulated Pd island. (a) Before a tip change. Depth of the depressions is \sim 90 pm. (b) Tip changed at the arrow. (c) After the tip change. Depth of the depression is \sim 32 pm. These depressions are attributed to single Pd atoms. Images were recorded at 0.8 nA and 1.0 V.

growth of the vacancy pits next to the islands, such as seen in Figure 3. The Ag atoms migrate to the top of the islands through a hopping ascent. The barrier for a hopping descent is lower than for ascent as there is greater coordination in the final state for descent than for ascent. However, the barrier for ascent is lower if there is already a Ag atom on top of the island that the ascending Ag atom can bond to. Our STM images are consistent with the idea that the presence of second-layer atoms serves to nucleate further growth of the second layer. Exchange can also place a Pd atom into the second layer, creating a second-layer PdAg alloy.

We see evidence of isolated Pd atoms on the second layer in the images of Figure 8. This is consistent with our previous RAIRS study of CO on Pd/Ag(111) in which we continued to detect CO adsorbed on Pd atop sites (but not Pd bridge sites) after annealing to temperatures where the first-layer Pd islands should have been completely covered by a second layer. Evidence for layer-by-layer Pd dissolution (stage 4) is provided in the Supporting Information where after annealing 0.150 ML of Pd to 470 K, double-layer Ag islands are observed that were presumably on top of a Pd island that had dissolved into the substrate.

Our observations are generally consistent with the modeling of Lim et al.³ At room temperature we observe the result of processes occurring over periods of tens of minutes that they predict should occur at 500 K in a few microseconds. In cases where there is an overlap in experimental conditions, our images are also in agreement with the previously reported work. 2,4,19 The line profiles in Figure 5b show more corrugation than for the Ag(111) terraces, which is consistent with the structure seen most prominently in Figure 2c. Patel et al. observed somewhat similar lines in Pt and Pd islands on Ag(111), which they attributed to moiré structure associated with the lattice mismatch between the two elements. 13,19 More generally, dislocations can form to relieve the stress due to lattice misfit. The Ag lattice constant is only 5% greater than that of Pd. For lattice misfits of 9% or less, pseudomorphic growth of the first layer is expected.³⁰ This would place Pd atoms at the fcc 3-fold hollow sites of the Ag(111) terraces, such that the lattice constant of the 2D Pd islands would exactly match that of the Ag substrate and no moiré pattern or dislocation lines would be expected. In the case of Ag deposited onto Pd(111), pseudomorphic islands were formed at some Ag coverages, whereas dislocation lines were observed at other coverages. 28 Dislocation features were also observed in

Ag deposited onto Pt(111), where the lattice mismatch is even less. ^{31,32} For Ag on Pd(111) or Pt(111), the lattice mismatch for pseudomorphic islands leads to compressive stress, whereas it would be tensile stress for pseudomorphic Pd islands on Ag(111). The stress associated with expanding the Pd–Pd distances could be partly relieved by compressing the topmost Ag layer under the Pd islands, such that the lattice mismatch between the combined Pd island/topmost Ag layer could generate a moiré pattern. Lim et al. do not indicate if their Pd₉₁ islands have the lattice constant of Pd(111), Ag(111), or something in between.³ The structure seen in the Pd island could also be associated with mixing Ag atoms into the Pd layer in a nonrandom way. However, PdAg alloys that form for Ag deposited onto Pd(111) display a nearly random distribution.²⁸

Regardless of the origin of the structure seen in the Pd islands, the experiments reveal that this structure provides nucleation sites for the growth of a Ag layer. These sites appear to be generally located near the center of the islands. The observed structure was not included in the simulations of Lim et al.,3 and therefore this aspect of the encapsulation process was not addressed in their simulations. It might be possible to elucidate the structure through theoretical calculations of the most energetically favorable way to place Pd atoms onto the Ag(111) surface while also allowing one or more Ag layers to rearrange to their optimum positions. Periodic moiré-type patterns may then be obtained with certain sites found to be more favorable for the placement of second-layer Ag atoms. This would be similar to what is seem for metal deposition on graphene on metal surfaces. In the case of Ir deposited on graphene on Ir(111), special nucleation sites of the moiré lattice were observed experimentally with STM and theoretically described with DFT calculations.³³ In an early STM study of heteroepitaxial growth, it was also found that regular arrays of Ni islands formed at certain dislocation sites of the herringbone reconstruction of Au(111).³⁴

5. CONCLUSIONS

Low coverages of Pd deposited onto the Ag(111) surface at room temperature form small hexagonal islands consisting of a single layer of Pd. Because of the higher surface free energy of Pd, these structures are not thermodynamically stable. The kinetic barriers for Pd diffusion into the Ag bulk are high enough that the Pd remains on the surface indefinitely at room temperature. However, barriers for Ag migration from the

surface to the top of the Pd islands are low enough that Ag encapsulation of the Pd islands is observed to occur in minutes at room temperature. Scanning the surface after 48 h shows that a negligible amount of Ag encapsulation takes place at a Pd coverage of 0.024 ML, whereas 88% of the Pd islands were encapsulated at 0.150 ML of Pd. Nevertheless, 98% of the Pd islands are encapsulated by Ag upon annealing to 340 K, regardless of the coverage. However, upon further annealing we observed that the composition of some islands at a coverage of 0.150 ML of Pd changed to Ag/Ag/Pd/Ag(111). The migration of the Ag atoms to the top of the Pd islands leads to the formation of vacancy pits in the Ag(111) terraces. These observations agree with those reported in earlier STM studies and are consistent with the results of molecular dynamics simulations. The dislocation-type structure observed on the Pd islands provides nucleation sites for the growth of the second Ag layer. Annealing to 470 K and above results in the disappearance of Pd and restoration of a flat Ag(111) surface.

ASSOCIATED CONTENT

Supporting Information

The Supporting Information is available free of charge at https://pubs.acs.org/doi/10.1021/acs.jpcc.1c08736.

Additional STM images under different conditions, including those obtained by annealing 0.064 and 0.150 ML of Pd to the same temperatures as used in Figure 7 (PDF)

AUTHOR INFORMATION

Corresponding Author

Michael Trenary — Department of Chemistry, University of Illinois at Chicago, Chicago, Illinois 60607, United States; orcid.org/0000-0003-1419-9252; Phone: 312 996-0777; Email: mtrenary@uic.edu; Fax: 312 996-0431

Authors

Buddhika S. A. Gedara – Department of Chemistry, University of Illinois at Chicago, Chicago, Illinois 60607, United States

Mark Muir – Department of Chemistry, University of Illinois at Chicago, Chicago, Illinois 60607, United States

Arephin Islam — Department of Chemistry, University of Illinois at Chicago, Chicago, Illinois 60607, United States; orcid.org/0000-0001-8528-859X

Dairong Liu − Department of Chemistry, University of Illinois at Chicago, Chicago, Illinois 60607, United States;
orcid.org/0000-0002-9569-8207

Complete contact information is available at: https://pubs.acs.org/10.1021/acs.jpcc.1c08736

Notes

The authors declare no competing financial interest.

ACKNOWLEDGMENTS

We gratefully acknowledge financial support from the National Science Foundation (CHE-2102622). We thank Prof. E. Charles H. Sykes for making unpublished STM images of Pd/Ag(111) available to us and for valuable discussions.

■ REFERENCES

- (1) Zhang, Q.; Li, J.; Liu, X.; Zhu, Q. Synergetic Effect of Pd and Ag Dispersed on Al₂O₃ in the Selective Hydrogenation of Acetylene. *Appl. Catal., A* **2000**, *197*, 221–228.
- (2) van Spronsen, M. A.; Daunmu, K.; O'Connor, C. R.; Egle, T.; Kersell, H.; Oliver-Meseguer, J.; Salmeron, M. B.; Madix, R. J.; Sautet, P.; Friend, C. M. Dynamics of Surface Alloys: Rearrangement of Pd/Ag(111) Induced by CO and O₂. *J. Phys. Chem. C* **2019**, *123*, 8312–8323.
- (3) Lim, J. S.; Vandermause, J.; van Spronsen, M. A.; Musaelian, A.; Xie, Y.; Sun, L.; O'Connor, C. R.; Egle, T.; Molinari, N.; Florian, J.; Duanmu, K.; Madix, R. J.; Sautet, P.; Friend, C. M.; Kozinsky, B. Evolution of Metastable Structures at Bimetallic Surfaces from Microscopy and Machine-Learning Molecular Dynamics. *J. Am. Chem. Soc.* **2020**, *142*, 15907–15916.
- (4) O'Connor, C. R.; Duanmu, K.; Patel, D. A.; Muramoto, E.; van Spronsen, M. A.; Stacchiola, D.; Sykes, E. C. H.; Sautet, P.; Madix, R. J.; Friend, C. M. Facilitating Hydrogen Atom Migration via a Dense Phase on Palladium Islands to a Surrounding Silver Surface. *Proc. Natl. Acad. Sci. U. S. A.* **2020**, *117*, 22657.
- (5) Muir, M.; Trenary, M. Adsorption of CO to Characterize the Structure of a Pd/Ag(111) Single-Atom Alloy Surface. *J. Phys. Chem.* C **2020**, *124*, 14722–14729.
- (6) Horcas, I.; Fernandez, R.; Gomez-Rodriguez, J. M.; Colchero, J.; Gomez-Herrero, J.; Baro, A. M. WSXM: A Software for Scanning Probe Microscopy and a Tool for Nanotechnology. *Rev. Sci. Instrum.* **2007**, *78*, 013705.
- (7) Cox, E.; Li, M.; Chung, P.-W.; Ghosh, C.; Rahman, T. S.; Jenks, C. J.; Evans, J. W.; Thiel, P. A. Temperature Dependence of Island Growth Shapes During Submonolayer Deposition of Ag on Ag(111). *Phys. Rev. B: Condens. Matter Mater. Phys.* **2005**, 71, 115414.
- (8) Davey, W. P. Precision Measurements of the Lattice Constants of Twelve Common Metals. *Phys. Rev.* **1925**, *25*, 753–761.
- (9) Lewandowski, M.; Pabisiak, T.; Michalak, N.; Milosz, Z.; Babačić, V.; Wang, Y.; Hermanowicz, M.; Palotás, K.; Jurga, S.; Kiejna, A. On the Structure of Ultrathin FeO Films on Ag(111). *Nanomaterials* **2018**, *8*, 828.
- (10) Resta, A.; Leoni, T.; Barth, C.; Ranguis, A.; Becker, C.; Bruhn, T.; Vogt, P.; Le Lay, G. Atomic Structures of Silicene Layers Grown on Ag(111): Scanning Tunneling Microscopy and Noncontact Atomic Force Microscopy Observations. *Sci. Rep.* **2013**, *3*, 2399.
- (11) Gao, W.; Baker, T. A.; Zhou, L.; Pinnaduwage, D. S.; Kaxiras, E.; Friend, C. M. Chlorine Adsorption on Au(111): Chlorine Overlayer or Surface Chloride? *J. Am. Chem. Soc.* **2008**, *130*, 3560–3565.
- (12) Reinert, F.; Nicolay, G. Influence of the Herringbone Reconstruction on the Surface Electronic Structure of Au(111). *Appl. Phys. A: Mater. Sci. Process.* **2004**, *78*, 817–821.
- (13) Patel, D. A.; Kress, P. L.; Cramer, L. A.; Larson, A. M.; Sykes, E. C. H. Elucidating the Composition of PtAg Surface Alloys with Atomic-Scale Imaging and Spectroscopy. *J. Chem. Phys.* **2019**, *151*, 164705.
- (14) de la Figuera, J.; Prieto, J. E.; Ocal, C.; Miranda, R. Surface Etching and Enhanced Diffusion During the Early Stages of the growth of Co on Cu(111). *Surf. Sci.* **1994**, 307–309, 538–543.
- (15) Rabe, A.; Memmel, N.; Steltenpohl, A.; Fauster, T. Room-Temperature Instability of Co/Cu(111). *Phys. Rev. Lett.* **1994**, 73, 2728–2731.
- (16) An, B.; Wen, M.; Zhang, L.; Imade, M.; Iijima, T.; Fukuyama, S.; Yokogawa, K. Atomic Structure of Interface Between Monolayer Pd Film and Ni(111) Determined by Low-Energy Electron Diffraction and Scanning Tunneling Microscopy. *J. Appl. Phys.* **2010**, *108*, 103521.
- (17) Blecher, M. E.; Lewis, E. A.; Pronschinske, A.; Murphy, C. J.; Mattera, M. F. G.; Liriano, M. L.; Sykes, E. C. H. Squeezing and Stretching Pd thin films: A High-Resolution STM Study of Pd/Au(111) and Pd/Cu(111) Bimetallics. *Surf. Sci.* **2016**, 646, 1–4.

- (18) Terada, S.; Yokoyama, T.; Saito, N.; Okamoto, Y.; Ohta, T. Growth and Moiré Superstructure of Palladium Films on Ni(111) Studied by STM. Surf. Sci. 1999, 433–435, 657–660.
- (19) Patel, D. A. Atomic-Scale Insights in the Surface Structure and Reactivity of Model Catalytic Surfaces: Towards the Design of Sustainable Catalysts, Tufts University, 2020.
- (20) Schouteden, K.; Amin-Ahmadi, B.; Li, Z.; Muzychenko, D.; Schryvers, D.; Van Haesendonck, C. Electronically Decoupled Stacking Fault Tetrahedra Embedded in Au(111) Films. *Nat. Commun.* **2016**, *7*, 14001.
- (21) Schouteden, K.; Van Haesendonck, C. Lateral Quantization of Two-Dimensional Electron States by Embedded Ag Nanocrystals. *Phys. Rev. Lett.* **2012**, *108*, 076806.
- (22) Lucci, F. R.; Lawton, T. J.; Pronschinske, A.; Sykes, E. C. H. Atomic Scale Surface Structure of Pt/Cu(111) Surface Alloys. *J. Phys. Chem. C* 2014, *118*, 3015–3022.
- (23) Bellisario, D. O.; Han, J. W.; Tierney, H. L.; Baber, A. E.; Sholl, D. S.; Sykes, E. C. H. Importance of Kinetics in Surface Alloying: A Comparison of the Diffusion Pathways of Pd and Ag Atoms on Cu(111). *J. Phys. Chem. C* **2009**, *113*, 12863–12869.
- (24) Tierney, H. L.; Baber, A. E.; Sykes, E. C. H. Atomic-Scale Imaging and Electronic Structure Determination of Catalytic Sites on Pd/Cu Near Surface Alloys. *J. Phys. Chem. C* **2009**, *113*, 7246–7250.
- (25) Wang, Y.; Papanikolaou, K. G.; Hannagan, R. T.; Patel, D. A.; Balema, T. A.; Cramer, L. A.; Kress, P. L.; Stamatakis, M.; Sykes, E. C. H. Surface Facet Dependence of Competing Alloying Mechanisms. *J. Chem. Phys.* **2020**, *153*, 244702.
- (26) Nagl, C.; Haller, O.; Platzgummer, E.; Schmid, M.; Varga, P. Submonolayer Growth of Pb on Cu(111): Surface Alloying and De-Alloying. *Surf. Sci.* **1994**, 321, 237–248.
- (27) Tyson, W. R.; Miller, W. A. Surface Free Energies of Solid Metals: Estimation from Liquid Surface Tension Measurements. *Surf. Sci.* 1977, 62, 267–276.
- (28) Engstfeld, A. K.; Hoster, H. E.; Behm, R. J. Formation, Atomic Distribution and Mixing Energy in Two-Dimensional Pd_xAg_{1-x} Surface Alloys on Pd(111). *Phys. Chem. Chem. Phys.* **2012**, *14*, 10754–10761.
- (29) Michely, T.; Hohage, M.; Bott, M.; Comsa, G. Inversion of Growth Speed Anisotropy in Two Dimensions. *Phys. Rev. Lett.* **1993**, 70, 3943–3946.
- (30) Frank, F. C.; Van Der Merwe, J. H.; Mott, N. F. One-Dimensional Dislocations. II. Misfitting Monolayers and Oriented Overgrowth. *Proc. R. Soc. London, Ser. A* **1949**, 198, 216–225.
- (31) Bromann, K.; Brune, H.; Giovannini, M.; Kern, K. Pseudomorphic Growth Induced by Chemical Adatom Potential. *Surf. Sci.* 1997, 388, L1107–L1114.
- (32) Hamilton, J. C.; Stumpf, R.; Bromann, K.; Giovannini, M.; Kern, K.; Brune, H. Dislocation Structures of Submonolayer Films near the Commensurate-Incommensurate Phase Transition: Ag on Pt(111). *Phys. Rev. Lett.* **1999**, *82*, 4488–4491.
- (33) N'Diaye, A. T.; Bleikamp, S.; Feibelman, P. J.; Michely, T. Two-Dimensional Ir Cluster Lattice on a Graphene Moiré on Ir(111). *Phys. Rev. Lett.* **2006**, *97*, 215501.
- (34) Chambliss, D. D.; Wilson, R. J.; Chiang, S. Nucleation of Ordered Ni Island Arrays on Au(111) by Surface-Lattice Dislocations. *Phys. Rev. Lett.* **1991**, *66*, 1721–1724.

